Analytica Chimica Acta 953 (2017) 40–47

Contents lists available at ScienceDirect

Analytica Chimica Acta

journal homepage: www.elsevier.com/locate/aca

Integrated work-flow for quantitative metabolome profiling of plants, Peucedani Radix as a case

Yuelin Song [a, 1], Qingqing Song [a, b, 1], Yao Liu [a, b], Jun Li [a], Jian-Bo Wan [c], Yitao Wang [c], Yong Jiang [d, **], Pengfei Tu [a, *]

[a] Modern Research Center for Traditional Chinese Medicine, Beijing University of Chinese Medicine, Beijing, 100029, China
[b] School of Chinese Materia Medica, Beijing University of Chinese Medicine, Beijing, 100102, China
[c] State Key Laboratory of Quality Research in Chinese Medicine, Institute of Chinese Medical Sciences, University of Macau, Taipa, 999078, Macao
[d] State Key Laboratory of Natural and Biomimetic Drugs, School of Pharmaceutical Sciences, Peking University, Beijing, 100191, China

HIGHLIGHTS

- Novel three-step workflow was proposed for non-targeted metabolomics.
- Optimal collision energy was firstly utilized for the discrimination of isomers.
- Linear ranges were extended by suppressing the responses with inferior parameters.
- Authentic compound-free method was implemented for parameter optimization.
- Universal quantitation was achieved by a set of diluted herbal extract mixture.

GRAPHICAL ABSTRACT

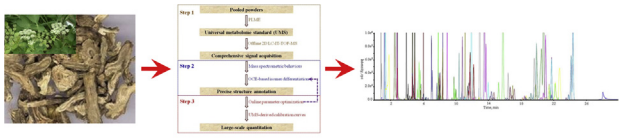

ARTICLE INFO

Article history:
Received 1 August 2016
Received in revised form
7 November 2016
Accepted 21 November 2016
Available online 3 December 2016

Keywords:
Quantitative metabolome
Integrated work-flow
Offline two dimensional liquid chromatography
Linear range
Peucedani Radix
Isomer

ABSTRACT

Universal acquisition of reliable information regarding the qualitative and quantitative properties of complicated matrices is the premise for the success of metabolomics study. Liquid chromatography-mass spectrometry (LC-MS) is now serving as a workhorse for metabolomics; however, LC-MS-based non-targeted metabolomics is suffering from some shortcomings, even some cutting-edge techniques have been introduced. Aiming to tackle, to some extent, the drawbacks of the conventional approaches, such as redundant information, detector saturation, low sensitivity, and inconstant signal number among different runs, herein, a novel and flexible work-flow consisting of three progressive steps was proposed to profile in depth the quantitative metabolome of plants. The roots of *Peucedanum praeruptorum* Dunn (Peucedani Radix, PR) that are rich in various coumarin isomers, were employed as a case study to verify the applicability. First, offline two dimensional LC-MS was utilized for in-depth detection of metabolites in a pooled PR extract namely universal metabolome standard (UMS). Second, mass fragmentation rules, notably concerning angular-type pyranocoumarins that are the primary chemical homologues in PR, and available databases were integrated for signal assignment and structural annotation. Third, optimum collision energy (OCE) as well as ion transition for multiple monitoring reaction measurement was online optimized with a reference compound-free strategy for each annotated component and large-scale

* Corresponding author.
** Corresponding author.
E-mail addresses: yongjiang@bjmu.edu.cn (Y. Jiang), pengfeitu@163.com (P. Tu).
[1] These two authors contribute equally to this article.

http://dx.doi.org/10.1016/j.aca.2016.11.066
0003-2670/© 2016 Elsevier B.V. All rights reserved.

relative quantification of all annotated components was accomplished by plotting calibration curves *via* serially diluting UMS. It is worthwhile to highlight that the potential of OCE for isomer discrimination was described and the linearity ranges of those primary ingredients were extended by suppressing their responses. The integrated workflow is expected to be qualified as a promising pipeline to clarify the quantitative metabolome of plants because it could not only holistically provide qualitative information, but also straightforwardly generate accurate quantitative dataset.

© 2016 Elsevier B.V. All rights reserved.

1. Introduction

Sustainable efforts are being devoted by numerous analysts from all over the world to develop a practical liquid chromatography-mass spectrometric (LC-MS) approach for metabolomics being capable of universally and reliably acquiring information regarding the qualitative and quantitative properties of the complicated matrices [1]. Conventional LC-MS methodologies for non-targeted metabolomics usually suffer from: 1) redundant information resulted from in-source collision induced dissociation (CID) and adduct ions (*e.g.* $[M+Na]^+$, $[M+HCOO]^-$); 2) the reliability of the replacement of concentration with peak area because of the unsatisfactory dynamic ranges of LC-MS [2]; 3) biased mass spectrometric responses partially attributing to the challenge of applying appropriate parameters for each metabolite in a single run; and 4) unsatisfactory reproducibility resulted from inconsistent detection signal numbers as well as imperfect peak alignment parameters during data processing. On the other side, the poor coverage for metabolome and the requirement of authentic compounds are the inherent disadvantages of targeted metabolomics, indicating that it cannot act as a survey tool to comprehensively gain information. Recently, pseudo-targeted metabolomics and stable-isotope labeling pipeline have been proposed by Xu's [3–5] and Li's [6–9] groups, respectively, to tackle the cons of the untargeted term. However, some unsatisfactory points still remain. For instance, primary amine, secondary amine, or phenolic hydroxyl group is mandatory for isotope labeling, whilst the pseudo-targeted metabolomics is still disadvantageous at the confidence of each quantitative variable in the dataset of given samples. Herein, an attempt was made to address, to some extent, the shortcomings of those existing protocols, and an integrated work-flow (Fig. 1) was proposed to clarify the quantitative metabolome of plants. The roots of *Peucedanum praeruptorum* Dunn that are a famous medicinal material named Peucedani Radix (PR) and rich in various coumarin isomers, were employed as a proof-of-concept to verify the applicability of the flexible work-flow.

Firstly, offline two dimensional LC coupled with hybrid ion trap-time of flight MS (2D LC-IT-TOF-MS) was implemented for in-depth characterization of metabolites in a pooled PR extract namely universal metabolome standard (UMS) [10]. Secondly, mass fragmentation rules, notably concerning angular-type pyranocoumarins that are the primary chemical homologues in PR [11], were integrated with some available databases for signal assignment and structural annotation. Thirdly, optimum collision energy (OCE) as well as ion transition for multiple monitoring reaction (MRM) measurement was online optimized with a reference compound-free approach for each annotated component and large-scale relative quantification of all annotated identities, including three unknown compounds, was accomplished by plotting calibration curves *via* serially diluting UMS. Moreover, OCE was highlighted because of its potential for isomer discrimination, and the linearity ranges of those primary compounds were extended by suppressing the responses through deliberately applying inferior parameters or ion transitions. We envision that the integrated workflow could act as a practical tool for non-targeted metabolomics of plants, as well as some other complicated matrices, because of its potential for universally acquiring qualitative and quantitative information of given samples.

2. Experimental

2.1. Materials and chemicals

Eleven batches of Peucedani Radix (PR1–PR11) were collected from different habitats in China and authenticated by one of the authors (Prof. P.F. Tu), whereas four batches of Angelicae dahuricae Radix, consisting of the dried roots of *Angelica dahurica* (AD1–AD4), were collected to serve as the fakes. All voucher specimens are deposited in the herbarium of our institute and their detailed information is elucidated in Table S1 (Supplemental information A). All crude materials were dried using a universal oven with forced convection at 40 °C and pulverized with a mill, and the powders were then griddled through a 50 mesh sieve.

LC-MS grade formic acid, methanol, and acetonitrile (ACN) were purchased from Thermo-Fisher (Pittsburgh, PA, USA). Deionized water was prepared using a Milli-Q purification system (Millipore, Bedford, MA, USA). Analytical grade methanol was supplied by Xilong Scientific (Shantou, Guangdong, China). 1,2,3,7-tetramethoxyxanthone served as an internal standard (IS) and was obtained from the chemical library of the State Key Laboratory of Natural and Biomimetic Drugs, Peking University (Beijing,

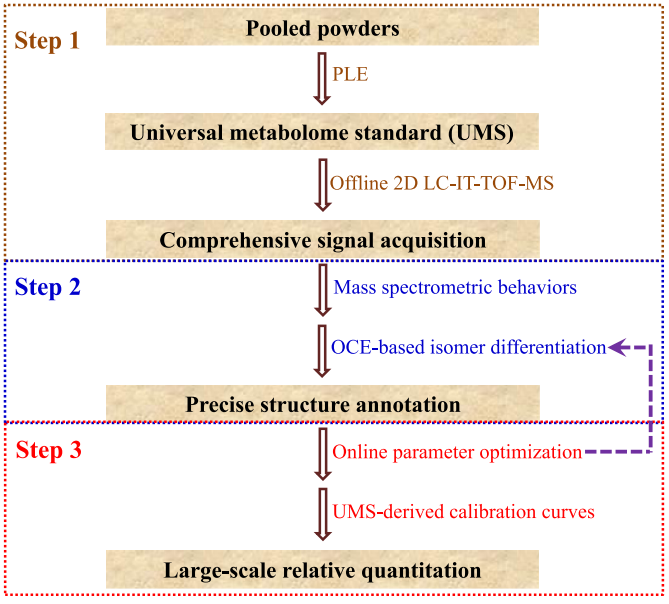

Fig. 1. Brief schematic of the newly proposed work-flow for quantitative metabolome profiling of Peucedani Radix.

China). Diatomaceous earth was the product of Celite Standard Super-cel (Shanghai, China).

2.2. Apparatus

All liquid chromatographic separations were conducted on a Shimadzu LC-20AD LC system, consisting of two LC-20AD$_{XR}$ pumps, a SIL-20AC$_{XR}$ auto-sampler, a CTO-20AC column oven, a DGU-20A$_{3R}$ degasser, a SPD-M20A DAD module along with a CBM-20A controller (Shimadzu, Kyoto, Japan). A hybrid ion trap-time of flight-mass spectrometer (IT-TOF-MS, Shimadzu, Kyoto, Japan) equipped with an electronic spray ionization (ESI) interface was employed to provide high-resolution tandem mass spectra, whereas a hybrid triple quadrupole-linear ion trap mass spectrometer (Qtrap-MS, ABSciex 5500, Foster City, CA, USA) equipped with a Turbo V™ ESI interface was responsible for quantitative measurement. Quantitative ^{1}H NMR spectroscopy was carried out on a Varian UNITY plus 500 MHz spectrometer (VNMR500, Varian Inc., Palo Alto, CA, USA) at 499.91 MHz proton frequency equipped with TCI cryoprobe and *Z*-gradient system, and defaulted parameters were applied for spectral acquisition.

2.3. Comprehensive signal acquisition using offline 2D LC-IT-TOF-MS

Aliquots (10 mg for each batch) of all pulverized PR materials were pooled, and a portion (accurately weighed as 5.00 mg) of the mixture was thoroughly dispersed with clean diatomaceous earth (approximately 10 mg). The mixed powders were subjected into a home-made extraction vessel that was composed of a hollow guard column (3.0 × 4.0 mm, Phenomenex, Torrance, CA, USA) and a suitable cartridge, and the inlet and outlet of the extraction vessel were then connected with a LC-20AD$_{XR}$ pump (Shimadzu, Kyoto, Japan) and a long PEEK tube (0.13 × 1000 mm, Agilent Technologies, Santa Clara, CA, USA), respectively, to carry out miniaturized pressurized liquid extraction (PLE) following the protocols described in the literature [12–14]. The effluent was collected at the outlet of the long PEEK tube. Extraction parameters were set as below: solvent, methanol; temperature, 75 °C; flow rate, 2.5 mL/min; and duration, 3 min. The collection (7.5 mL in total) was concentrated to residues with a rotary evaporator and reconstituted with 150 μL of methanol to afford UMS solution. A 100 μL aliquot of UMS solution was loaded onto a Waters Xbridge Amide column (4.6 × 150 mm, 3.5 μm, Milford, CT, USA) according to ten parallel injections. The column was maintained at room temperature (20 °C) and chromatographic elution was carried out with 0.1% aqueous formic acid (A) and ACN containing 0.1% formic acid (B) following a gradient elution program as below: 0–5 min, 98% B; 5–8 min, 98–96% B; 8–14 min, 96–94% B; 14–16 min, 94–93% B; 16–18 min, 93–92% B; 18–20 min, 92–91% B; 20–25 min, 91–84% B; 25–32 min, 84–70% B; 32–34 min, 70–50% B; 34–35 min, 50% B; 35–36 min, 50–98% B; 36–45 min, 98% B; and flow rate, 0.8 mL/min to afford sixteen fractions in Eppendorf tubes (Hamburg, Germany) following the collection program illustrated in Fig. S1A (Supplemental information B). The effluent was monitored at 320 nm. Each fraction was concentrated to dryness with a gentle stream of nitrogen gas in a 40 °C water bath, and the residues were then separately reconstituted with 50 μL of methanol. Afterwards, a 5 μL aliquot of each solution was loaded onto a CAPCELL CORE C$_{18}$ column (2.1 × 150 mm, 2.7 μm, Shiseido, Tokyo, Japan) to carry out the second dimensional separation (Fig. S1B). Gradient elution with aforementioned solvents followed a program as follows: 0–12 min, 15–60% B; 12–18 min, 60–70% B; 18–20 min, 70–90% B; 20.1–25 min, 15% B; and flow rate, 0.4 mL/min. The column was maintained at 35 °C. The outlet of the CAPCELL CORE C$_{18}$ column was successively connected to DAD module (UV length, 320 nm) and IT-TOF-MS, the key parameters of which were set as the descriptions in the literature [15].

2.4. Online parameter optimization

High resolution mass spectral data were carefully analyzed to exclude the redundant information, such as adduct ions together with in-source CID-initiated fragment ion species, as well as substrate signals, nonetheless, to assign those effective information to putative identities.

Because it was impossible to obtain authentic compounds for all putative identities (Table S2, Supplemental information A), an authentic compound-independent strategy [16] was introduced for the optimizations of MRM ion transition, decluserting potential (DP), and CE. LC coupled with Qtrap-MS participated in online parameter tuning. To obtain satisfactory retention both hydrophilic components and hydrophobic substances, a robust Supelco Ascentis® Express F5 column (2.1 × 150 mm, 2.7 μm, Sigma-Aldrich, Bellefonte, DE, USA) filled with pentafluorophenylpropyl-bonded silica particles, was employed for chromatographic separation, and gradient elution was conducted with above solvents as follows: 0–4 min, 0–25% B; 4–10 min, 25–43% B; 10–15 min, 43% B; 15–18 min, 43–45% B; 18–22 min, 45–50% B; 22–26 min, 50–60% B; 26.1–30 min, 0% B; and flow rate, 0.4 mL/min. Injection volume for the F5 column was maintained at 2 μL.

Regarding parameter optimization, briefly, precursor ions (including quasi-molecular ions and adduct ions) and their primary fragment ion species for each compound in UMS, which were acquired by IT-TOF-MS, were seriatim paired to generate a series of MRM ion transition candidates, and each ion transition candidate then gave birth to serial pseudo ion transitions (PITs). PITs of each ion transition candidate corresponded to the staggered CEs (range: 5–60 eV; step-size: 1 eV) or declustering potentials (DPs, range: 30–200 eV; step-size: 10 V) levels. CE and DP of each ion transition candidate were optimized by scheduling those PITs into monitoring list [16]. The optimal parameter (OCE or optimum DP) or MRM ion transition was defined as the one corresponding to the greatest peak area for each analyte.

Taking a pair of *regio*-isomers, praeruptorin A *vs.* pteryxin, as representative cases, their sodium adduct ion, ammonium adduct ion, and protonated molecular ion were detected at *m/z* 409, 404, and 387, respectively, while the dominant fragment ion species of *m/z* 409 were observed as *m/z* 349, 327, 309, 245, and 227. Similar MS^2 spectra were also observed for the other two precursor ions, *e.g. m/z* 404 and 387. Therefore, several MRM ion transition candidates were generated, such as *m/z* 409 > 245, 409 > 227, 404 > 245, 404 > 227, *etc*. Afterwards, taking *m/z* 409 > 227 as a case, PITs were produced as *m/z* 409.000 > 227.000, 409.001 > 227.000, *etc*., exactly corresponding to those staggered CE values (*e.g.* 5, 6, 7, *etc*.), and then typed into the monitoring list to circumvent the self-inspection of Analyst software (Version 1.6.2, ABSciex). Scheduled MRM algorithm that could decrease the number of concurrent ion transitions by automatically assigning all MRM transitions into their expected retention time window was employed in response to the dramatically increased ion transitions [16]. The detection time window for each ion transition was set as 60 s (retention time ± 30 s), and the target scan time was maintained at 1.0 s. Because unit resolution (0.6–0.8 Da) was applied for either Q1 or Q3 chamber, those quadropole mass analyzers could not, actually, discriminate PITs; however, PITs could yield different responses because of their different CEs. The area of each PIT was tagged with corresponding CE value and transmitted into Microsoft Office Excel. A peak area *vs.* CE curve was plotted for each ion transition candidate of each analyte, for instance *m/z* 409 > 227 for

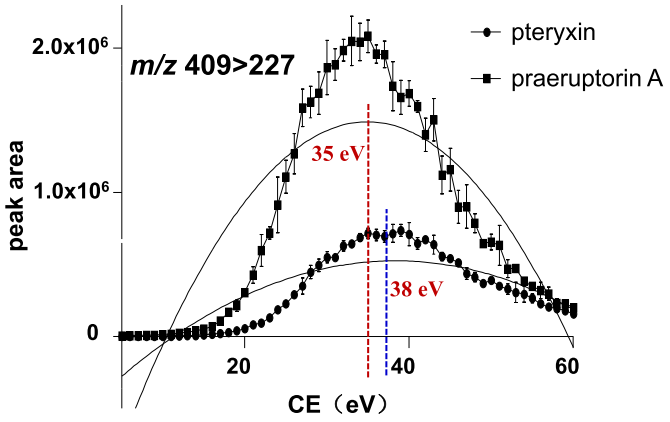

Fig. 2. Peak area-CE trajectories and the fitted parabolas of praeruptorin A (square) and pteryxin (dot). The OCEs of praeruptorin A and pteryxin were calculated as 35 eV and 38 eV, respectively, corresponding to the vertexes of the parabolas ($y = -2516\ x^2 + 175439x - 1557000$ and $y = -715.7\ x^2 + 54947x - 530218$ for praeruptorin A and pteryxin, respectively).

praeruptorin A, and OCE was calculated using the regressive binomial formula (Fig. 2). Following CE optimization, DPs were optimized with the same manner, however, among the range of 30–200 V (*e.g.* 40, 50, 60, *etc.*).

2.5. Validation of quantitative method

Afterwards, those optimized ion transitions, OCEs, and optimum DPs were typed into the monitoring table of scheduled MRM mode.

Method validation was carried out for all annotated 92 compounds (Table S2) in terms of linearity, sensitivity, intra- and inter-day, repeatability, stability, recovery, and matrix effect [17]. UMS solution was sequentially diluted with methanol to afford a set of diluted solutions such as 1000 × , 500 × , 200 × , 100 × , 50 × , 25 × , 10 × , and 5 × , and each obtained solution (200 μL) was further 2-fold diluted by thoroughly mixing with equal volume of IS solution (500 ng/mL in methanol) to yield serial calibration samples.

When those acquired data were subjected into the quantitative module of Analyst software (ABSciex, Foster City, CA, USA), satisfactory linearity could not obtain for those primary components in UMS, such as praeruptorin A, pteryxin, praeruptorin B, and praeruptorin E because of the saturation for the sensor located at the back of Q3 chamber. Therefore, an attempt was made to suppress the generation of the fragment ions that finally reached at the sensor, through modifying parameters, in particular CE. Taking praeruptorin B as an example, dilution levels of 50 × , 25 × , 10 × , and 5 × were obviously located away from the theoretical calibration curve (Fig. 3A) when OCE (14 eV) was applied for *m/z* 444 > 327; hence, an inferior CE as 36 eV was utilized to extend the linear range to 5 × . Following the replacement of OCEs with appropriate CEs for those primary ingredients, those calibration samples were re-analyzed and the calibration curves were reconstructed. Lower limit of quantitation (LOQ) of each analyte corresponded to the greatest dilution level of the linear range for each analyte, whereas limit of detection (LOD) of each analyte corresponded to the certain dilution level that generated the signal with signal to noise ratio (S/N) about 3.

Calibration samples of low (500 ×), medium (50 ×), and high (10 ×) dilution levels were selected as quality control (QC) samples to assess the intra-day and inter-day precisions following the descriptions in the literature [17]. All the variations were expressed with the relative standard deviations (RSDs%) of the peak area

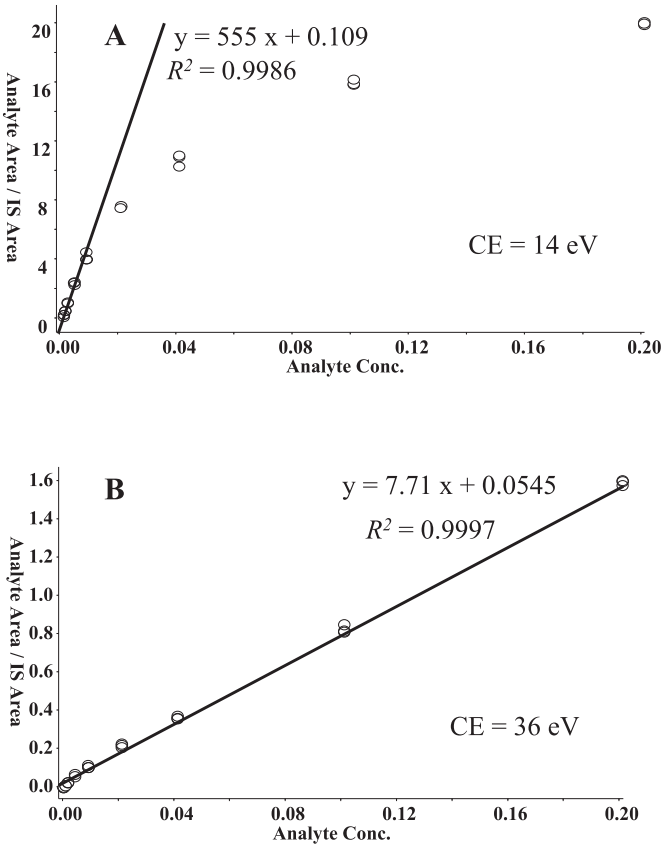

Fig. 3. **A**, With the employment of the OCE of praeruptorin B (14 eV for *m/z* 444 > 327), four dilution levels (5 × , 10 × , 25 × , and 50 ×) obviously located away from the theoretical curve ($y = 555x + 0.109$, $R^2 = 0.9986$); **B**, With the employment of the modified CE (36 eV), satisfactory linearity were observed for all dilution levels ($y = 7.71x + 0.0545$, $R^2 = 0.9997$).

ratios between targeted analytes and internal standard.

A well-defined approach [18] was introduced for matrix effect assay. In brief, a selected sample (PR8) instead of methanol was used to dilute UMS solution to yield serial concentration levels, such as 1000 × , 500 × , 200 × , 100 × , 50 × , 25 × , 10 × , and 5 × , and the obtained solutions were further fortified with IS solution and subjected for calibration curve plotting. The slope of the new calibration curve of each analyte was compared with the slope of that obtained above to calculate the signal suppression/enhancement (SSE), which was used for quantitative assessment of the matrix effects, according to the following equation defined by Sulyok et al. [19]: $SSE = slope_{spiked\ extract}/slope_{liquid\ standard} \times 100\%$.

Regarding recovery assay, diluted UMS solutions with appropriate concentrations were spiked into selected sample (PR8) whose quantitative profile was clarified, *via* an auto-sampler as previous descriptions [12–14], and the collections were then assayed in parallel with the crude materials. The recovery was calculated with the following equation: recovery (%) = (amount found − original amount)/amount spiked × 100%. Moreover, PR8 was also utilized for repeatability and stability assays using the protocols archived in the literature [17].

On the other side, each accurately weighed (approximately 5.00 mg) sample (PR1–PR11 & AD1–AD4) was subjected for PLE [12–14]. Parameters for the generation of UMS were applied and 7.5 mL of effluent was collected for each sample. After that a 100 μL aliquot of each collection was 50-fold diluted with methanol, a 200 μL aliquot of the obtained solution was then fortified with equal volume (200 μL) of IS solution (500 ng/mL in methanol).

Afterwards, the prepared samples were introduced for quantitative analysis, and each measurement was conducted in triplicate. A selected QC sample (50 × calibration sample) was inserted into the analysis batch after every three measurements.

2.6. Statistical analysis

The dataset of PR1–PR11 and AD1–AD4 as well as those selected QC samples (50 × calibration sample) was imported from Analyst software as a ".csv" file. Principal component analysis (PCA) was performed using SIMCA-P v14.0 software (Umetrics, Umeå, Sweden) after that all variables were Pareto-scaled.

3. Results and discussion

3.1. Signal acquisition and putative structure identification

To advance the extraction efficiency for the pooled PR powders, a robust home-made PLE module [12–14] was introduced to yield UMS that is expected to contain all metabolites in 11 batches and PR samples. In order to assess the extraction efficiency, a microwave-assisted extraction (MAE) manner was introduced for comparison. The experimental conditions that described in our previous article [11] were applied to process PR8. Then, certain volume of the MAE product, corresponding to equal pulverized materials with that of PLE sample, was subjected for LC-Qtrap-MS measurement using those optimized parameters. Afterwards, the chromatograms obtained for MAE and PLE were directly overlayed, and the results indicated that the extraction outcomes of PLE were slight more than, as expected, that yielded by MAE.

Because offline 2D LC-MS has been widely demonstrated as a favored approach to characterize in depth the chemical profiles of given complicated matrices [20–22], this integrated tool was thereby implemented to afford greater peak capacity as well as to expose those minor components in UMS in comparison of single column LC-MS. Given the great orthogonality between hydrophilic interaction chromatography (HILIC) and reverse phase (RP) modes [23,24], a Waters Xbridge Amide column and a CAPCELL CORE C_{18} column were finally employed to carry out the first and second separation dimensions, respectively, following careful evaluations among several candidates. Elution program for either dimension was carefully optimized to obtain satisfactory chromatographic performances. S/N as 100 was adopted as the criterion for signal filtering. As a result, a total of 89 compounds, including 81 coumarins, four amino acids (*e.g.* valine, leucine, isoleucine, and glutamic acid), and four nucleosides (*e.g.* cytidine, uridine, adenosine, and guanosine), were putatively identified *via* matching with those proposed mass fragmentation pathways [11,25] (Fig. S2, Supplemental information B), and referring to the accessible databanks, such as MassBank (http://www.massbank.jp), HMDB (http://www.hmdb.ca), ChemSpider (www.chemspider.com), and MyCompoundID (http://www.mycompoundid.org/mycompoundid_IsoMS/index.jsp), whereas three signals were assigned as unknown compounds (**8**, **11** and **14**). The information concerning signal assignment of all compounds is illustrated in Table S2.

3.2. Parameter optimization and precise structure annotation

Authentic compounds were generally required by MRM-based quantification for plotting the calibration curves along with compound-dependent parameters optimization, in particular OCE; however, it was impossible to collect enough amounts of pure authentic compounds for all detected signals transmitted from the chemical profiling of complicated matrices. Therefore, a useful authentic compound-free strategy was introduced to obtain optimum parameters for all identities.

A brief schematic for the principle of online parameter optimization strategy is illustrated in Fig. S3 (Supplemental information B). In theory, each peak observed in MRM chromatogram was plotted from serial data points, and each data point was acquired in a single cycle time that was the sum of dwell times for all experiments along with intervals. Regarding a single acquisition cycle, all PITs were individually monitored corresponding to their unique parameters. Afterwards, a peak can be plotted for every PIT, and all peak shapes should be consistent with the chromatographic behaviour of the selected analyte. To ensure the assignment of enough dwell time for each PIT, scheduled MRM algorithm was applied for guaranteeing the reproducibility of parameter optimization.

The optimum MRM ion transitions were obtained by directly comparing responses, whereas OCEs or optimal DPs were gained by plotting peak area *vs*. CE (or DP) trajectories. In comparison of CE and ion transition, the contribution of DP for mass response was quite minor. Fig. 2 elucidates the OCEs for pteryxin (**60**) and praeruptorin A (**62**) as 38 eV and 35 eV, respectively, whereas the optimal MRM ion transition for either was gained as *m/z* 409 > 227. All optimized parameters and ion transitions of all analytes are summarized in Table S2.

It was always difficult to discriminate isomers, notably *regio*-isomers. Generally speaking, every compound possesses unique physicochemical parameters, unless enantiomers (*e.g. d*-praeruptorin A *vs. l*-praeruptorin A) the discrimination of which was beyond the scope of our current study; hence, differences could widely occur among various compounds, even *regio*-isomers and diastereoisomers, in regard of either chromatographic or spectrometric behaviours. In sight of the different OCEs between a pair of *regio*-isomers, praeruptorin A *vs*. pteryxin (Fig. 2), OCE might serve as a pivotal clue for precise structure annotation. Therefore, those aforementioned putative identities for the components in UMS were re-evaluated to strengthen structural identification. Actually, PR is rich in various isomers, for instance, praeruptorin A *vs*. pteryxin, as well as *cis*/*trans*-khellactone (**13**&**17**) *vs*. qianhucoumarin G (**20**). Firstly, given the discrimination of the mass cracking patterns between angular-type pyranocoumarins and linear-furanocoumarins [25], the differentiation of those isomers could be easily achieved. Taking *cis/trans*-khellactone *vs.* qianhucoumarin G for instance, *m/z* 175.03 $[M+H-C_3H_8O-H_2O]^+$ was observed as the diagnostic fragment ion species for qianhucoumarin G rather than *cis/trans*-khellactone. Furthermore, OCE of qianhucoumarin G (17 eV) was different from that of *cis/trans*-khellactone (27 eV/24 eV) when an identical ion transition (*m/z* 263 > 245) was applied for all of them. Regarding praeruptorin A *vs.* pteryxin, an angeloyloxy group instead of an acetyloxy group existed at C-4′ of pteryxin; therefore, a larger and stronger intra-molecular conjugated system could be formed, indicating that greater CE level was required to dissociate the C-4′–*O* bond of pteryxin [26]. Therefore, it was not surprising that OCE value (*m/z* 409 > 227) of pteryxin (38 eV) was mildly greater than that of praeruptorin A (35 eV) (Fig. 2). Such 3 eV variance was also found for another ion transition candidates between this pair of isomers, including ammonium adduct ion-to-dominant fragment ions (*m/z* 404 > 245 and 404 > 227) and sodium adduct ion-to-primary fragment ion (*m/z* 409 > 245). Moreover, an attempt was also carried out to tentatively assign the signals to *cis*-khellactone and *trans*-khellactone. Because the hydroxyl group of *trans*-khellactone shared a plane with the coumarin substructure and an intra-molecular conjugated system could be generated, the hydrophilicity thereby increased and the C-4′–*O* bond exhibited greater bond energy than that of *cis*-khellactone. Hence, *trans*-khellactone (OCE, 24 eV; t_R, 4.69 min) showed greater OCE value (ion transition, *m/z* 263 > 245), yet lower retention time

than *cis*-khellactone (OCE, 27 eV; t_R, 4.95 min). In addition, identical tandem mass spectral profiles were observed for compounds **12** and **15**, both of which were tentatively identified as khellactone-3′-*O*-glycoside [27]; however, OCEs for their ion transition (*m/z* 442 > 263) were optimized as 20 eV and 25 eV for compounds **12** and **15**, respectively. Because the hydroxyl group at C-4′ site might affect the dissociation of the glycoside bond at C-3′ site, in particular for *cis*-configuration; hence, the OCE of *cis*-configurational isomer should be 25 eV. Fortunately, the elution order of praeroside III (**12**; t_R, 4.64 min) and II (**15**; t_R, 4.93 min) agreed well with their hydrophilicity that was partially governed by C-4′-OH moiety. Although great efforts were made, in current study, to discriminate the isomers whose minor differences only occurred at the substitutes, for instance, the replacement of angeloyl group with tigloyl or senecioyl moiety; however, none significant variation was observed for OCEs among such isomers.

3.3. Method validation

After obtaining optimized parameters as well as appropriate gradient elution program for the versatile F5 column [28], scheduled MRM technique [29] was employed to simultaneously monitor those ion transitions belonging to all 92 analytes. Regarding MRM-based quantification, authentic compounds were usually required for plotting calibration curves to achieve the transformation of peak area to content. However, absolute quantification was not mandatory, actually, for comparative metabolomics study [3–5], because comparative metabolomics primarily focused on the comparison between different sample groups. Consequently, serially diluted UMS was implemented to generate calibration curves and then to relatively quantify all analytes in PR1–PR11, and the obtained contents were defined as quasi-contents.

Although MRM mode on Qtrap-MS was believed to be able of measuring analytes covering large concentration ranges in complex samples because of its relatively wide linear dynamic range that spanned four orders of magnitude [30], saturation could still occur for the sensor located at the back of Q3 chamber, which limited the linear range and made the accurate quantification of metabolites with concentrations across several orders of magnitude challenging. Although optimal parameters could guarantee the sensitive detection of those minor components, it was still of great importance to extend the linearity ranges for those primary components in PR, such as praeruptorin A, praeruptorin B, and praeruptorin E. A feasible way was decreasing the counts of fragment ions that finally arrived at the sensor, according to employing inferior parameters or ion transitions. Praeruptorin B (**81**) was selected as a representative compound to illustrate this smart operation. UMS was serially diluted to generate a calibration curve for each analyte by plotting the peak area ratios (y) between selected analyte and IS *vs.* dilution levels (x). With the employment of OCE (14 eV for *m/z* 444 > 327), four dilution levels (5 ×, 10 ×, 25 ×, and 50 ×) obviously located away from the theoretical curve of praeruptorin B ($y = 555x + 0.109$, $R^2 = 0.9986$, Fig. 3A). It is thereby necessary to suppress the mass response for at least 50-fold. CE as 36 eV was thereby applied for praeruptorin B because the intensity corresponding to 36 eV was merely 2% of that afforded by OCE (14 eV). Afterwards, the calibration curve was reconstructed by assaying those calibration samples with the modified CE (36 eV). As expected, the linearity range was extended as from 1000 × to 5 × (linearity equation: $y = 7.71x + 0.0545$, $R^2 = 0.9997$, Fig. 3B). Moreover, the linearity ranges of some other primary components, including praeruptorin A, praeruptorin E, pteryxin, *etc*. were also extended by modifying CEs to match with their primary distributions in PR. The information regarding the appropriate ion transitions, CEs, and DPs are summarized in Table S2 and those primary components employing inferior CEs are marked with the symbol "*". The chromatogram of UMS is exhibited in Fig. 4. Calibration curves (Table S3, Supplemental information A) indicated good linearity ($R^2 > 0.99$) over the corresponding linear concentration range, from 500 × to 5 × for most analytes.

The RSDs% of intra- and inter-day precisions were among 1.44–17.7% and 1.37–17.8% for all 92 analytes, respectively. Concerning repeatability assay, RSDs% of 53% and 86% of analytes were less than 5% and 10%, respectively. Regarding the stability, 90% of analytes exhibited RSDs% less than 10% (Table S3). Recovery assay was carried out by spiking diluted UMS solutions into a selected sample (PR8), and all recoveries ranged from 80.05% to 125.94% with RSDs% lower than 20% (Table S3). The protocols previously proposed [18] were followed for matrix effect assays, and two sets of calibration curves were obtained. The SSE values were calculated among 81.4–120.7%, indicating that none significant matrix effect occurred for all analytes. Together, the developed method could fulfil the criteria for simultaneously relative quantification of all 92 components in PR.

3.4. In-depth characterization of quantitative metabolome of PR

The validated method was applied for the clarification of the quantitative metabolome of PR. The datasets containing all quasi-contents of all analytes in PR1–PR11 were subjected for principle component analysis. Moreover, the datasets belonging to those QC samples (50-fold diluted UMS), as well as the fakes (AD1–AD4)

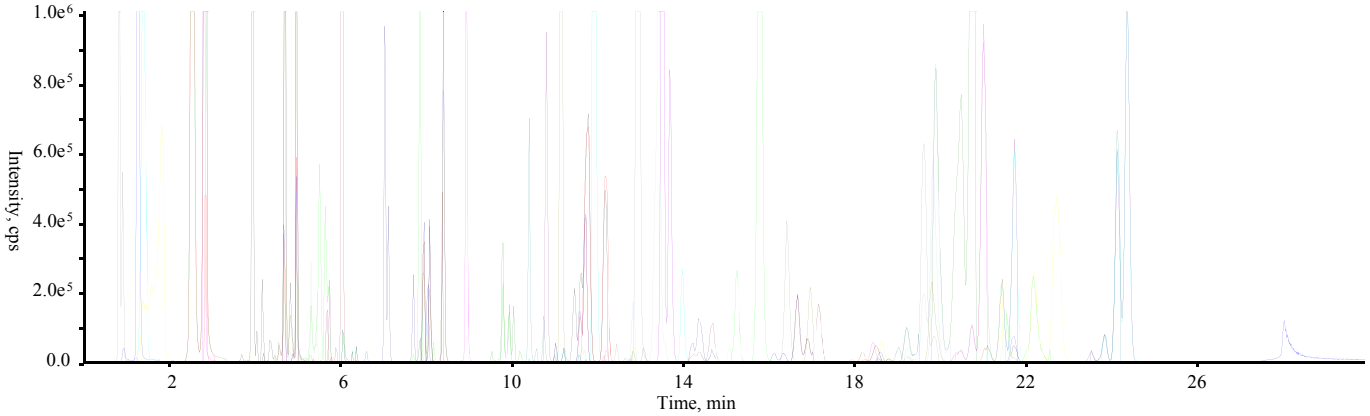

Fig. 4. Overlaid extract ion current chromatogram (92 MRM ion transitions) for the quantitative metabolome of UMS.

were also exported into SIMCA-P software. As shown in Fig. S4A (Supplemental information B), the dots corresponding to QC samples tightly gathered, whereas dots of the fakes were scattered at the edge of the 95% confidence interval. To highlight the differences among PR samples from different habitats, the dots corresponding to those fakes were removed and re-modelling was performed. The QC sample dots still clustered with most PR samples, whereas PR1, PR3, PR9, and PR10 were distributed away from the other dots (Fig. S4B, Supplemental information B), suggesting that the quantitative metabolome of those four batches was quite different from the other ones.

Although none authentic compound (except internal standard), was implemented, quasi-contents of all analytes were gained using the proposed work-flow. To cross-validate the results, two methods, including an authentic compound-free NMR-based quantification [31] and an authentic compound-dependent LC-MS [11] were employed by following the protocols in the literature. Absolute quantification of thirteen coumarins in UMS and PR1–PR11 were carried out using LC-MS [11]. And the contents of praeruptorin A and praeruptorin B in those samples were also obtained by comparing the integral values of quantitative signals with the signals yielded by an internal standard (formononetin) using quantitative ^{1}H NMR spectroscopy [31]. Representative ^{1}H NMR ($CDCl_3$, 500 MHz) spectrum is shown in Fig. S5 (Supplemental information B). Selected signals, including 2-H (δ 7.96, s) of formononetin, 4′-H (δ 6.68, *d*, $J = 5.0$ Hz) of praeruptorin B, and 4′-H (δ 6.57, *d*, $J = 5.0$ Hz) of praeruptorin A were utilized for quantitative analysis. Fortunately, great consistence was observed among those three sets (including the new work-flow) of quantitative results, indicating the newly proposed method to be reliable.

In addition, those authentic isomers documented in our previous article [11] as well as the eight hydrophilic references [29], including valine, leucine, isoleucine, glutamic acid, cytidine, uridine, adenosine, and guanosine, were injected into LC-MS system to match with the signals in the chromatogram of UMS, and the reasonability of the putative identification was confirmed. Those OCEs as well as optimal ion transitions provided with the online optimization strategy exhibited a great consistence with those afforded by manual tuning [11].

To further confirm the utility of OCE for isomer discrimination, two pairs of *regio*-isomers that were generated from the incubation of praeruptorin A with rat liver microsomes following previous descriptions [32], were involved. Fortunately, greater (3 eV) OCEs were observed for *cis*-4′-acetylkhellactone and *cis*-4′-angeloylkhellactone than those of *cis*-3′-acetylkhellactone and *cis*-3′-angeloylkhellactone, respectively, attributing to the higher energy of C-4′-*O* bond than C-3′–*O* bond. Above all, OCE could act as an important role for isomer discrimination.

The aforementioned four drawbacks of conventional protocols were addressed, to some extent, with the new work-flow. Each component exactly corresponded to one variable (quasi-content) in the component table, whilst the redundant information was filtrated *via* structural annotation. Praeruptorin A as a case, all primary signals observed in MS^1 spectrum, such as *m/z* 425, 409, 404, 387, 327, 245, and 227 that might play roles in data processing of non-targeted metabolomics was solely replaced with ion transition of *m/z* 409 > 227. Reliable quasi-contents instead of peak areas were obtained for all analytes *via* plotting calibration curves by diluting UMS. Biased mass responses could also be circumvented, to some extent, because of the employment of optimal parameters for minor components yet inferior parameters for primary ones. The dataset of LC-scheduled MRM could be conveniently imported into SIMCA-P software without any alignment process, because all analytes were tagged with retention times along with identities and all samples had the identical component table. Moreover, scheduled MRM could allow simultaneously monitoring of as many as one thousand ion transitions on Qtrap-MS equipment without sacrificing the data quality [33]. This work-flow could be conveniently combined with some other preferred metabolomics methods, such as stable-isotope labeling method and pseudo-targeted metabolomics, as well as data mining approaches for LC-MS/MS dataset, *e.g.* diagnostic fragment ion and mass defect filtering, to promote the success of metabolomics.

4. Conclusions

In conclusion, a robust and flexible work-flow was proposed to clarify the quantitative metabolome of PR. Firstly, comprehensive signal acquisition was guaranteed by integrating orthogonal HILIC and RP-LC, as well as IT-TOF-MS. Precise structure annotation was subsequently achieved by referring to those well-defined mass fragmentation patterns along with available databases, and OCE firstly served as an important role for *regio*-isomers differentiation. Finally, holistically relative quantification was accomplished by developing an authentic compound-independent method. The applicability of the work-flow was demonstrated by the performance of metabolomics for a panel of PR samples. Together, the workflow can serve as a promising methodology to characterize in depth the quantitative metabolome of plants, as well as some other complicated matrices (*e.g.* biological samples, foods, beverages, *etc.*), because it could not only holistically provide qualitative information, but also straightforwardly generate accurate quantitative information.

Acknowledgements

This work was financially supported by National Science Fund of China (Nos. 81403073 and 81530097), Quality guarantee system of Chinese herbal medicines (No. 201507002), and foundation from Beijing University of Chinese Medicine (Nos. 2016-JYB-XJQ004 and 2016-JYB-XS090).

Appendix A. Supplementary data

Supplementary data related to this article can be found at http://dx.doi.org/10.1016/j.aca.2016.11.066.

References

[1] R.A. Dixon, D. Strack, Phytochemistry meets genome analysis, and beyond, Phytochemistry 62 (2003) 815–816.
[2] M. Bantscheff, M. Schirle, G. Sweetman, J. Rick, B. Kuster, Quantitative mass spectrometry in proteomics: a critical review, Anal. Bioanal. Chem. 389 (2007) 1017–1031.
[3] S. Chen, H. Kong, X. Lu, Y. Li, P. Yin, Z. Zeng, G. Xu, Pseudotargeted metabolomics method and its application in serum biomarker discovery for hepatocellular carcinoma based on ultra high-performance liquid chromatography/triple quadrupole mass spectrometry, Anal. Chem. 85 (2013) 8326–8333.
[4] Y. Li, Q. Ruan, Y. Li, G. Ye, X. Lu, X. Lin, G. Xu, A novel approach to transforming a non-targeted metabolic profiling method to a pseudo-targeted method using the retention time locking gas chromatography/mass spectrometry-selected ions monitoring, J. Chromatogr. A 1255 (2012) 228–236.
[5] P. Luo, W. Dai, P. Yin, Z. Zeng, H. Kong, L. Zhou, X. Wang, S. Chen, X. Lu, G. Xu, Multiple reaction monitoring-ion pair finder: a systematic approach to transform nontargeted mode to pseudotargeted mode for metabolomics study based on liquid chromatography-mass spectrometry, Anal. Chem. 87 (2015) 5050–5055.
[6] D. Achaintre, A. Bulete, C. Cren-Olive, L. Li, S. Rinaldi, A. Scalbert, Differential isotope labeling of 38 dietary polyphenols and their quantification in urine by liquid chromatography electrospray ionization tandem mass spectrometry, Anal. Chem. 88 (2016) 2637–2644.
[7] J. Peng, K. Guo, J. Xia, J. Zhou, J. Yang, D. Westaway, D.S. Wishart, L. Li, Development of isotope labeling liquid chromatography mass spectrometry for mouse urine metabolomics: quantitative metabolomic study of transgenic mice related to Alzheimer's disease, J. Proteome Res. 13 (2014) 4457–4469.

[8] W. Xu, D. Chen, N. Wang, T. Zhang, R. Zhou, T. Huan, Y. Lu, X. Su, Q. Xie, L. Li, L. Li, Development of high-performance chemical isotope labeling LC-MS for profiling the human fecal metabolome, Anal. Chem. 87 (2015) 829–836.
[9] X. Su, N. Wang, D. Chen, Y. Li, Y. Lu, T. Huan, W. Xu, L. Li, L. Li, Dansylation isotope labeling liquid chromatography mass spectrometry for parallel profiling of human urinary and fecal submetabolomes, Anal. Chim. Acta 903 (2016) 100–109.
[10] J. Peng, Y.T. Chen, C.L. Chen, L. Li, Development of a universal metabolome-standard method for long-term LC-MS metabolome profiling and its application for bladder cancer urine-metabolite-biomarker discovery, Anal. Chem. 86 (2014) 6540–6547.
[11] Y.L. Song, W.H. Jing, G. Du, F.Q. Yang, R. Yan, Y.T. Wang, Qualitative analysis and enantiospecific determination of angular-type pyranocoumarins in Peucedani Radix using achiral and chiral liquid chromatography coupled with tandem mass spectrometry, J. Chromatogr. A 1338 (2014) 24–37.
[12] Q.Q. Song, J. Li, X. Liu, Y. Zhang, L.P. Guo, Y. Jiang, Y.L. Song, P.F. Tu, Home-made online hyphenation of pressurized liquid extraction, turbulent flow chromatography, and high performance liquid chromatography, *Cistanche deserticola* as a case study, J. Chromatogr. A 1438 (2016) 189–197.
[13] Y.L. Song, Q.Q. Song, J. Li, S.P. Shi, L.P. Guo, Y.F. Zhao, Y. Jiang, P.F. Tu, Chromatographic analysis of Polygalae Radix by online hyphenating pressurized liquid extraction, Sci. Rep. 6 (2016) 27303.
[14] Y.L. Song, Q.Q. Song, J. Li, J. Zheng, C. Li, Y. Zhang, L. Zhang, Y. Jiang, P.F. Tu, An integrated platform for directly widely-targeted quantitative analysis of feces part I: platform configuration and method validation, J. Chromatogr. A 1454 (2016) 58–66.
[15] J. Sun, Y.L. Song, J. Zhang, Z. Huang, H.X. Huo, J. Zheng, Q. Zhang, Y.F. Zhao, J. Li, P.F. Tu, Characterization and quantitative analysis of phenylpropanoid amides in eggplant (*Solanum melongena* L.) by high performance liquid chromatography coupled with diode array detection and hybrid ion trap time-of-flight mass spectrometry, J. Agric. Food Chem. 63 (2015) 3426–3436.
[16] Y.L. Song, Q.Q. Song, J. Li, J. Zheng, C. Li, Y. Zhang, L.L. Zhang, Y. Jiang, P.F. Tu, An integrated platform for directly widely-targeted quantitative analysis of feces part II: an application for steroids, eicosanoids, and porphyrins profiling, J. Chromatogr. A 1460 (2016) 74–83.
[17] G. Du, H.Y. Zhao, Q.W. Zhang, G.H. Li, F.Q. Yang, Y. Wang, Y.C. Li, Y.T. Wang, A rapid method for simultaneous determination of 14 phenolic compounds in Radix Puerariae using microwave-assisted extraction and ultra high performance liquid chromatography coupled with diode array detection and time-of-flight mass spectrometry, J. Chromatogr. A 1217 (2010) 705–714.
[18] G. Du, H.Y. Zhao, Y.L. Song, Q.W. Zhang, Y.T. Wang, Rapid simultaneous determination of isoflavones in Radix puerariae using high-performance liquid chromatography-triple quadrupole mass spectrometry with novel shell-type column, J. Sep. Sci. 34 (2011) 2576–2585.
[19] M. Sulyok, F. Berthiller, R. Krska, R. Schuhmacher, Development and validation of a liquid chromatography/tandem mass spectrometric method for the determination of 39 mycotoxins in wheat and maize, Rapid Commun. Mass Spectrom. 20 (2006) 2649–2659.
[20] W. Sun, L. Tong, J. Miao, J. Huang, D. Li, Y. Li, H. Xiao, H. Sun, K. Bi, Separation and analysis of phenolic acids from *Salvia miltiorrhiza* and its related preparations by off-line two-dimensional hydrophilic interaction chromatography × reversed-phase liquid chromatography coupled with ion trap time-of-flight mass spectrometry, J. Chromatogr. A 1431 (2016) 79–88.
[21] W. Yang, J. Zhang, C. Yao, S. Qiu, M. Chen, H. Pan, X. Shi, W. Wu, D. Guo, Method development and application of offline two-dimensional liquid chromatography/quadrupole time-of-flight mass spectrometry-fast data directed analysis for comprehensive characterization of the saponins from Xueshuantong Injection, J. Pharm. Biomed. Anal. 128 (2016) 322–332.
[22] K. Li, Q. Fu, H. Xin, Y. Ke, Y. Jin, X. Liang, Alkaloids analysis using off-line two-dimensional supercritical fluid chromatography × ultra-high performance liquid chromatography, Analyst 139 (2014) 3577–3587.
[23] Y.M. Wang, J.Q. Zhao, J.L. Yang, Y.D. Tao, L.J. Mei, Y.P. Shi, Isolation and identification of saponins from the natural pasturage *Asterothamnus centrali-asiaticus* employing preparative two-dimensional reversed-phase liquid chromatography/hydrophilic interaction chromatography, J. Agric. Food Chem. 64 (2016) 4950–4957.
[24] J. Chen, L. Gao, Z. Li, S. Wang, J. Li, W. Cao, C. Sun, L. Zheng, X. Wang, Simultaneous screening for lipophilic and hydrophilic toxins in marine harmful algae using a serially coupled reversed-phase and hydrophilic interaction liquid chromatography separation system with high-resolution mass spectrometry, Anal. Chim. Acta 914 (2016) 117–126.
[25] Y. Tao, J. Luo, Y. Lu, D. Xu, Z. Hou, L. Kong, Rapid identification of two species of *Peucedanum* by high-performance liquid chromatography-diode array detection-electrospray ionization tandem mass spectrometry, Nat. Prod. Commun. 4 (2009) 1079–1084.
[26] Z.X. Chen, B.S. Huang, Q.L. She, G.F. Zeng, The chemical constituents of Bai-Hua-Qian-Hu, the root of *Peucedanum praeruptorum* Dunn. (Umbelliferae)–four new coumarins, Yao Xue Xue Bao 14 (1979) 486–496.
[27] M. Takata, T. Okuyama, S. Shibata, Studies on coumarins of a Chinese drug, "qian-hu"; VIII. Structures of new coumarin-glycosides of "bai-hua qian-hu", Planta Med. 54 (1988) 323–327.
[28] H. Yoshida, T. Mizukoshi, K. Hirayama, H. Miyano, Comprehensive analytical method for the determination of hydrophilic metabolites by high-performance liquid chromatography and mass spectrometry, J. Agric. Food Chem. 55 (2007) 551–560.
[29] Q.Q. Song, Y.L. Song, N. Zhang, J. Li, Y. Jiang, K.R. Zhang, Q. Zhang, P.F. Tu, Potential of hyphenated ultra-high performance liquid chromatography-scheduled multiple reaction monitoring algorithm for large-scale quantitative analysis of traditional Chinese medicines, RSC Adv. 5 (2015) 57372–57382.
[30] U. Vrhovsek, D. Masuero, M. Gasperotti, P. Franceschi, L. Caputi, R. Viola, F. Mattivi, A versatile targeted metabolomics method for the rapid quantification of multiple classes of phenolics in fruits and beverages, J. Agric. Food Chem. 60 (2012) 8831–8840.
[31] Y.L. Song, W.H. Jing, Y.G. Chen, Y.F. Yuan, R. Yan, Y.T. Wang, ^{1}H nuclear magnetic resonance based-metabolomic characterization of Peucedani Radix and simultaneous determination of praeruptorin A and praeruptorin B, J. Pharm. Biomed. Anal. 93 (2014) 86–94.
[32] Y.L. Song, W.H. Jing, H.Y. Zhao, R. Yan, P.T. Li, Y.T. Wang, Stereoselective metabolism of (+/-)-praeruptorin A, a calcium channel blocker from Peucedani Radix, in pooled liver microsomes of rats and humans, Xenobiotica 42 (2012) 231–237.
[33] Y.L. Song, Q.Q. Song, J. Li, N. Zhang, Y.F. Zhao, X. Liu, Y. Jiang, P.F. Tu, An integrated strategy to quantitatively differentiate chemome between *Cistanche deserticola* and *C. tubulosa* using high performance liquid chromatography-hybrid triple quadrupole-linear ion trap mass spectrometry, J. Chromatogr. A 1429 (2016) 238–247.